Failure of Quasi Brittle Materials Under Thermal Stress

J. W. Dougill

For materials that are not truly brittle, an alternative to a limiting stress criterion of failure is required. If an entire structural system is considered, failure can be taken to occur when the stiffness of the system is reduced so much that very large displacements could be caused by arbitrarily small increments of quasi static loading. This form of instability arises during unrestrained plastic flow. However, it can also occur because of gross changes in geometry and if the material has a descending portion in its stress/strain curve. The distinction between geometric and material instability is not clear, as it depends on the dimensional level of the investigation. Thus, macroscopic strain softening may be caused by significant changes in local geometry e.g. by necking of metallic bars in tension or through dilatency of granular materials.

The property of strain softening is intrinsic to materials that fail in a progressive manner with their stiffness being reduced by slow propagation of cracks or sequential breakage of bonds. Concrete, rocks and some ceramics behave in this way. In these materials, the effects of strain softening are evident from the instabilities that arise in compression tests using a flexible machine and the controlled behaviour observed in tests using stiff testing machines. However, the effects of strain softening are not always appreciated for other loadings. In particular, thermal loading provides a kind of strain controlled test,

on the material, in which the results are again dependent on the overall stiffness of the body and its supports.

To illustrate this, we consider a plane panel of a strain softening material that has the idealised properties given in the Table (fig. 1). We examine the behaviour when one face of the panel is suddenly exposed to high temperature.

Figure 1 compares the behaviour of two panels in which curvature is entirely inhibited. Here instability can occur only by a sudden change in the axial strain which occurs in the more heavily loaded panel after 8 min.48 sec. exposure. The bottom diagram in Figure 1 shows how the condition for instability is approached. The material adjacent to the heated face is driven over the top of the stress/strain curve, so increasing the size of the region of negative or zero stiffness, until the total longitudinal stiffness approaches zero.

With the less heavily loaded panel, tensile stresses are induced and cracking occurs next to the cooler face. The concomitant release of tensile stress causes some of the material in compression to unload and this reduces the size of the region of negative stiffness, as shown in the upper diagram of Figure 1. Here cracking is a stabilising influence and the panel survives although partly cracked.

Further results for flexurally restrained panels are shown in Figures 2 and 3. From these we see that higher exposure temperatures increase the range of loads for which instability can occur and that the time to failure is reduced as the descending branch of the stress/strain curve is made steeper. This is expected, as strain softening

represents behaviour that is intermediate between perfect plasticity, for which the load capacity would be unaffected by thermal stress, and brittle behaviour in which overall failure occurs as soon as the peak stress is achieved at one point.

For very low values of applied load, cracking can extend over most of the panel thickness. If this is regarded as failure, the range of loads that the panel can sustain and survive is restricted by a further limit of the form shown in Figure 2. Here, again the stiffness approaches zero, but in a gradual progressive manner.

Figure 4 shows results for the endurance of an axially restrained panel where instability occurs as pronounced curvature. Here high restraint causes early collapse but again it would be expected that some restraint would be required if progressive tensile failure was to be avoided.

Material instability is generally ignored in assessing the suitability of materials to resist thermal stress. Comparisons are often made on the basis of thermal stress resistance factors which are relevant to brittle behaviour and linear elastic materials but are seldom applicable to behaviour in compression. Clearly, compression failure must be regarded as a form of instability and any analysis must be conducted so as to reveal the unstable behaviour. Recognition of compression failure as a form of structural instability should lead to a better appreciation of the behaviour of materials and structures at high temperatures.

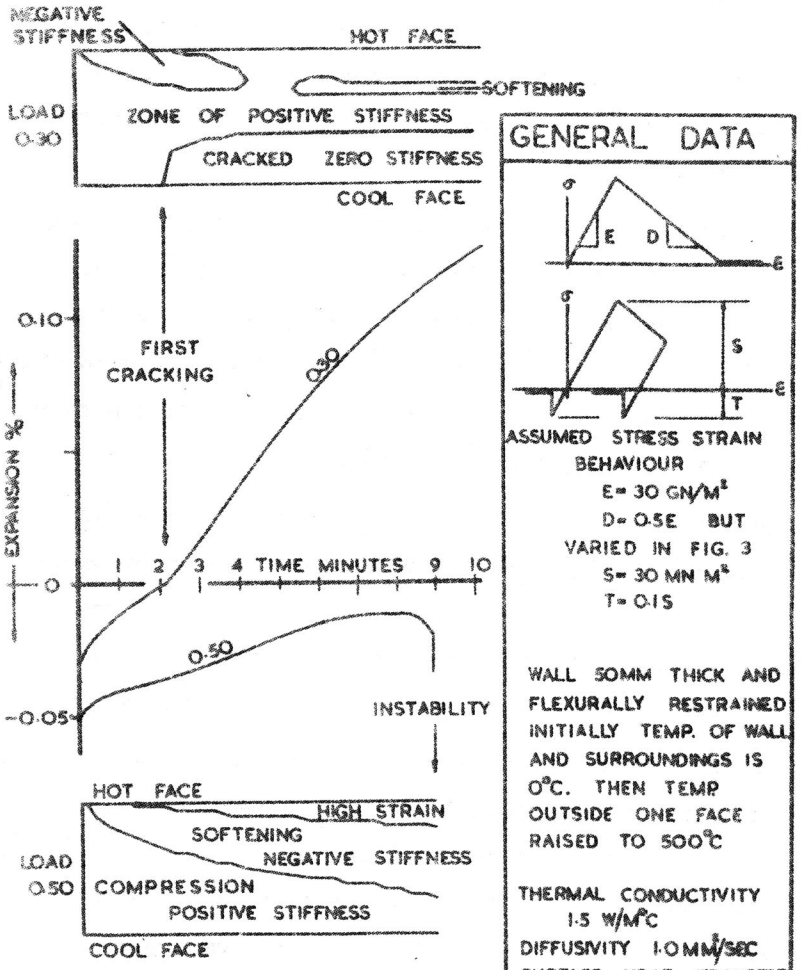

FIGURE 1 BEHAVIOUR OF FLEXURALLY RESTRAINED PANELS WITH AXIAL LOADS OF 30% AND 50% OF THE INITIAL LOAD CAPACITY

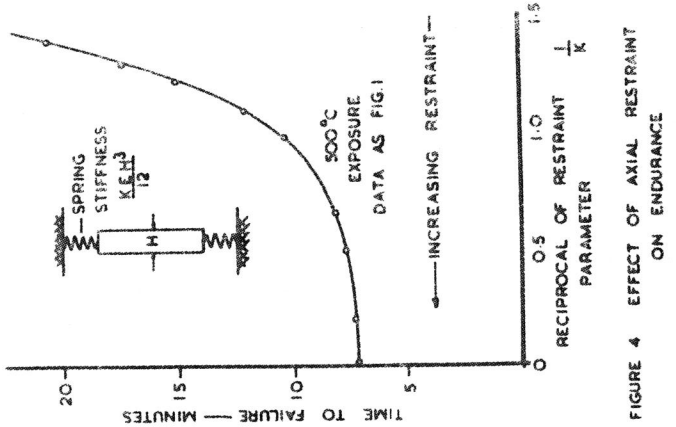

FIGURE 4 EFFECT OF AXIAL RESTRAINT ON ENDURANCE

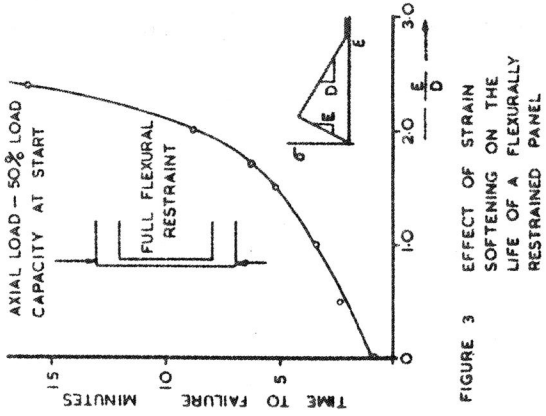

FIGURE 3 EFFECT OF STRAIN SOFTENING ON THE LIFE OF A FLEXURALLY RESTRAINED PANEL

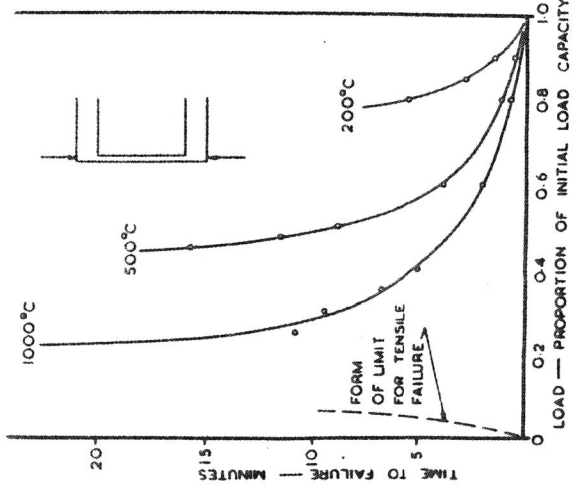

FIGURE 2 ENDURANCE OF FLEXURALLY RESTRAINED PANELS FOR A VARIETY OF LOADS AND AMBIENT TEMPERATURES

associated with crack extension. It will be shown that the solution obtained predicts K_{Ic} variations which correspond remarkably well with the observed effects.

Consider first the increase in strain energy, U, associated with the introduction of a semicircular crack ahead of a primary through crack (Fig. 1). A modification of Sack's[6] analysis shows that for large values of the ratio of the obstacle spacing to the obstacle diameter;[5]

$$U = \frac{8(1-\nu^2)}{3E} a^3\sigma^2 \left[1 + \frac{a'}{2a\sin\beta_o}\left[\frac{\pi}{2} + \frac{A/a}{\sqrt{1-A^2/a^2}} \ln\left(\frac{A/a(2+A/a-A^2/a^2)}{(A/a+1)(1+2\sqrt{1-A^2/a^2})}\right)\right]\right] + U_o \qquad (2)$$

where σ is the stress, E is Young's modulus, ν is Poisson's ratio, β_o is a constant, $A = r_o/\sin\beta_o$ and U_o is the contribution to the strain energy due to the cracked area between the obstacles. If it is now assumed, to a first approximation, that the crack shape does not change substantially during an increment da, in crack length, then the crack extension stress, σ_c, for a specimen of unit thickness, can be found from:

$$\zeta = \frac{dU}{dA} = \frac{1}{2}\frac{dU}{da} \qquad (3)$$

where ζ is the strain energy release rate ($K_1^2 = E\zeta$). Differentiating Eq. (2) with respect to a, and inserting in Eq. (3), gives:

$$\frac{\sigma_c^2}{\sigma_o^2} = \frac{3\pi^2 a'}{4(3a+a'(\pi+\Delta)/2\sin\beta_o)} \qquad (4)$$

where Δ is a function of a/r_o and σ_o is the stress to extend the primary crack in the absence of the obstacles. Solutions can also be obtained for small and intermediate a/r_o, by analytical and numerical integration, respectively. The results for all a/r_o are plotted graphically in Fig. 2 in terms of the ratio of K_{Ic} for the composite, K_{Ic}^c, and K_{Ic} for the matrix, K_{Ic}^m. (The critical shape of the crack at breakaway does not substantially

affect K_{Ic}[5], although the critical shape varies extensively with a/r_o, fig. 3). The cracks between adjacent obstacles will generally interact,[5] tending to reduce K_{Ic}^c ; the magnitude of this effect for spherical obstacles is shown in Fig. 2. Finally, the analysis assumes that the obstacles are impenetrable. In practice, penetration is likely to occur at a specific a/r_o[5], corresponding to a maximum in K_{Ic}^c (fig. 2).

3. IMPLICATIONS

The primary limitation of the analysis is the assumption that the crack shape does not change during crack extension, i.e. K_{Ic} is constant around the crack front. It is more likely that the stress intensity at the crack front will decrease in the x direction (Fig. 1), due to the stress field of the primary crack; although this may be partly counteracted by the impeding effect of the obstacle on the lateral motion of the crack. The limitations imposed by this assumption can only be assessed by comparing the predicted K_{Ic} variations with observed effects.

The analysis indicates that K_{Ic}^c should depend only on the ratio a/r_o, for a given obstacle shape. The available data[3,4] are plotted in this form in Fig. 4. The data (for obstacle impenetrability) can be fitted to a single curve without substantial deviations, thereby providing qualitative verification of the approach. The data are also compared with predicted variations for both interacting and non-interacting cracks (fig. 4). All of the data (for obstacle impenetrability) lie between these predicted variations, providing surprisingly good quantitative verification of the analytical solution. The deviation of the data above the interacting solution is probably due to the relative displacement of the crack front at the obstacles. The displacement is orthogonal to the original crack plane, and this impedes crack linking at the breakaway condition, as manifested by the formation of "cleavage trails."[7] This tends to increase K_{Ic}^c from the interacting solution towards the non-interacting solution.

The analysis also predicts that deviations below the interacting solution should occur at the onset of obstacle penetration. The results on the epoxy/alumina show this effect. The critical a/r_o for penetration decreases as the particle diameter decreases, implying perhaps that the smaller particles are weaker.

Finally, the results in Fig. 2 may be used to account for several microstructural effects on K_{Ic}. Spherical, intergranular porosity increases K_{Ic}[7], but the effect is likely to be smaller than indicated in Fig. 2, because the effective blocking diameter of a pore is less than the overall diameter. The relative K_{Ic} values in single and poly-crystals with anisotropic physical properties may also be partly explained by a crack blocking effect. For example, in plastically anisotropic materials the crack will be impeded at grains where the orientations are suitable for extensive plastic flow. The crack then bows between adjacent blocking grains and therefore enhances K_{Ic}.

REFERENCES

1. Brown, W.F., and Srawley, J.E., A.S.T.M., S.T.P. 410 (1967)
2. Lange, F.F., Phil. Mag., 22, 983 (1970).
3. Lange, F.F., and Radford, K.C., Jnl. Mater. Sci., 6, 1197(1971)
4. Lange, F.F., Jnl. Amer. Cerm. Soc., 54, 614(1971).
5. Evans, A.G., Phil. Mag., in press.
6. Sack, R.A., Proc. Phys. Soc., 58, 729(1946).
7. Passmore, E.M., Spriggs, R.M., and Vasilos, T., Jnl. Amer. Cerm. Soc., 48, 1 (1965).

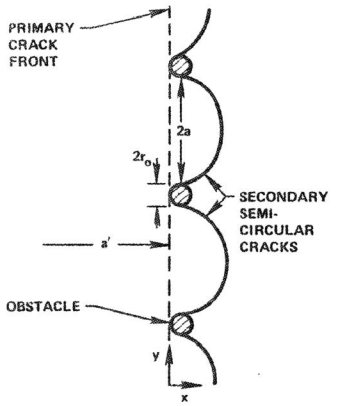

Figure 1.
The Formation of Secondary Cracks Between Obstacles at the Front of a Large Primary Through Crack

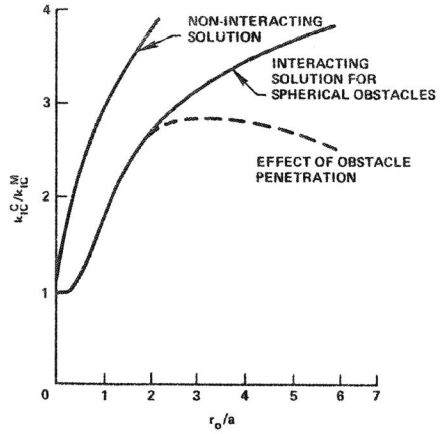

Figure 2.
Effect of Obstacle Spacing on the Stress Intensity Needed to Propagate a Crack Between Obstacles (Compared to the Matrix Value)

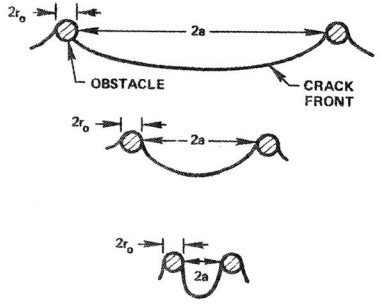

Figure 3.
Effect of Obstacle Spacing, a/r_o, on the Critical Crack Shape at Breakaway

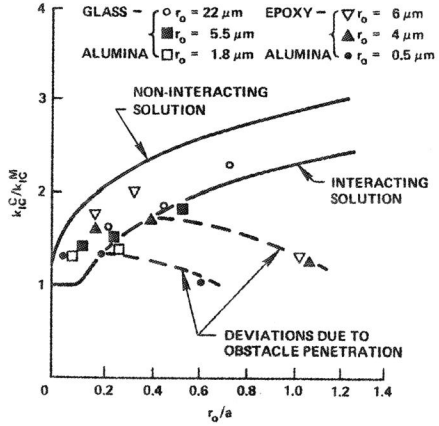

Figure 4.
Comparison of Available Data with Predicted k_{IC} Variations